

# SEA-LEVEL CHANGE: THE EXPECTED ECONOMIC COST OF PROTECTION OR ABANDONMENT IN THE UNITED STATES

GARY W. YOHE

*Department of Economics, Wesleyan University, Middletown, Connecticut 06459-6067, U.S.A.*

MICHAEL E. SCHLESINGER

*University of Illinois, Urbana-Champaign, 105 South Gregory Ave., Urbana, Illinois 61801, U.S.A.*

**Abstract.** Three distinct models from earlier work are combined to: (1) produce probabilistically weighted scenarios of greenhouse-gas-induced sea-level rise; (2) support estimates of the expected discounted value of the cost of sea-level rise to the developed coastline of the United States, and (3) develop reduced-form estimates of the functional relationship between those costs to anticipated sea-level rise, the cost of protection, and the anticipated rate of property-value appreciation. Four alternative representations of future sulfate emissions, each tied consistently to the forces that drive the initial trajectories of the greenhouse gases, are considered. Sea-level rise has a nonlinear effect on expected cost in all cases, but the estimated sensitivity falls short of being quadratic. The mean estimate for the expected discounted cost across the United States is approximately \$2 billion (with a 3% real discount rate), but the range of uncertainty around that estimate is enormous; indeed, the 10th and 90th percentile estimates run from less than \$0.2 billion up to more than \$4.6 billion. In addition, the mean estimate is very sensitive to associated sulfate emissions; it is, specifically, diminished by nearly 25% when base-case sulfate emission trajectories are considered and by more than 55% when high-sulfate trajectories are allowed.

## 1. Introduction

The threat of greenhouse-gas-induced sea-level rise has inspired many estimates of the potential economic cost since 1980. Table I makes this point by presenting estimates of the cost of either protecting or abandoning developed property in the United States for four projections of sea-level rise through the year 2100. Projections of the pace of rising seas that have been employed in exercises designed to estimate vulnerability and/or cost have, however, declined over recent years. Yohe (1989), for example, reported vulnerability estimates that he prepared for the United States Environmental Protection Agency along trajectories that ran from a low of 50 cm through 2100 up to 200 cm by that date. More recently, though, Fankhauser (1994) and Yohe et al. (1996) restricted their attention to scenarios that would see seas rise by no more than 100 cm through 2100. Indeed, their view is consistent with the most recent IPCC scenarios reported in Warrick et al. (1996) – scenarios that put the range of sea-level rise through 2100 between 20 cm and 90 cm.

Even for projected rises of 50 and 100 cm, though, cost estimates made before 1994 are about an order of magnitude higher than the most recent cost estimates. Earlier estimates missed: (a) the cost-reducing potential of market-based adaptation

*Climatic Change* **38**: 447–472, 1998.

© 1998 Kluwer Academic Publishers. Printed in the Netherlands.

in anticipation of the threat of rising seas; and/or (b) the efficiency of discrete decisions either to protect or abandon small tracts of property on a case-by-case basis using then-current evaluations of the benefits and cost of each. Estimates that incorporate both of these cost-reducing potentials (Fankhauser, 1994), however, still differ significantly due to alternative assumptions about the cost of protection and the value of property. Moreover, while trajectory-specific costs have maintained the interest of the policy community, none of the existing studies has taken the analysis to the point of offering estimates of the expected economic cost of protecting or abandoning property – estimates that are needed by that community.

This paper begins the process of meeting this need by reporting estimates of the expected cost of greenhouse-gas-induced sea-level rise to the developed coastline of the United States across a range of probabilistically weighted greenhouse-gas-emissions scenarios, including four alternative futures of anthropogenic sulfate aerosols created by emissions of sulfur dioxide, and it surrounds those estimates with 90 percent confidence intervals. Its results therefore push beyond the point estimates recorded in Table I for specific sea-level rise futures to offer estimates of the expected cost to the developed coastline of the United States and closed-form representations of how those costs vary with the cost of protection and the value of property. The estimates reported here are accomplished by: (1) identifying and characterizing probabilistically weighted emissions trajectories of greenhouse gases driven by global economic activity; (2) factoring these emissions trajectories into a simple climate/ocean model that calculates sea-level-rise trajectories across a range of climate sensitivities without and with associated anthropogenic sulfate emissions, the latter for specified anthropogenic sulfate aerosol (ASA) forcing; and (3) running the complete set of sea-level trajectories through the Yohe et al. (1996) costing model. The results include: (1) reduced-form estimates of the transient costs through the year 2100, expressed in terms of anticipated sea-level rise through that year; (2) estimates of the expected present value of the cost of sea-level rise along the developed coastline of the United States for various sulfate emission scenarios; and (3) 90% confidence intervals around these expected values that reflect both emissions uncertainties and estimation errors.

Section 2 describes the three models employed in this study, Section 3 presents the specific results, and Section 4 gives our conclusions.

## 2. The Models

Three separate models are employed sequentially to produce estimates of the functional relationship between the protection and abandonment costs attributable to rising seas along the developed United States coastline and the expected value of those costs across the full range of possible sea-level-rise futures. This section describes each model, in turn.

Table I

The potential cost of sea-level rise along the developed coastline of the United States (billions 1990\$). Source: Table 6 of Yohe et al. (1996)

Sea-level rise through 2100 and author(s)	(1) Context <sup>a</sup>	(2) Amortized <sup>b</sup>	(3) Cumulative <sup>c</sup>	(4) Transient (2065) <sup>d</sup>
<i>7.6 m</i>				
Schneider and Chen (1980)	Vulnerability	n/a	\$474	n/a
<i>4.6 m</i>				
Schneider and Chen (1980)	Vulnerability	n/a	\$347	n/a
<i>100 cm</i>				
Yohe (1989)	Vulnerability	n/a	\$321	\$1.37
Smith and Tirpak (1989)	Protection	n/a	\$73–\$111	n/a
Nordhaus (1991)	Protection	\$4.9	n/a	n/a
Cline (1992)	Protection	\$1.2	\$240	n/a
Fankhauser (1994)	Protection	\$1.0	\$62.6	n/a
Yohe et al. (1996)	Protection and abandonment	\$0.19	\$45.1	\$0.38
<i>50 cm</i>				
Yohe (1989)	Vulnerability	n/a	\$138	n/a
Cline (adjusted by Smith, 1996)	Protection	\$3.6	\$120	n/a
Fankhauser (1994)	Protection	\$0.57	\$35.6	n/a
Yohe et al. (1996)	Protection and abandonment	\$0.06	\$20.4	\$0.07

<sup>a</sup> Vulnerability measures the value of property (at the date of publication) that will be inundated by the year 2100. Protection denotes only the cost of protecting that property when protection is required. Abandonment reflects the current value of property, after anticipatory adaptation, at the time of inundation.

<sup>b</sup> Amortized values reflect the fixed annual value that produces a present value through the year 2100 equal to the cumulative values recorded in column (3).

<sup>c</sup> Cumulative values of costs or vulnerability estimates through the year 2100. They are undiscounted (except for Fankhauser). Fankhauser's estimates are discounted effectively by the annual rate of growth in per capita *GDP* (expected to average 1.6% for the U.S. through the year 2100).

<sup>d</sup> Transient costs are annual costs estimated to be incurred in a specific year – 2065 in this case. They are undiscounted.

## 2.1. GLOBAL ECONOMIC ACTIVITY TO EMISSIONS PROFILES

Most of the results reported here are drawn from an iterative global-emissions model designed to accommodate Monte Carlo simulation over multiple sources of uncertainty. Readers familiar with the lineage of integrated-assessment models will

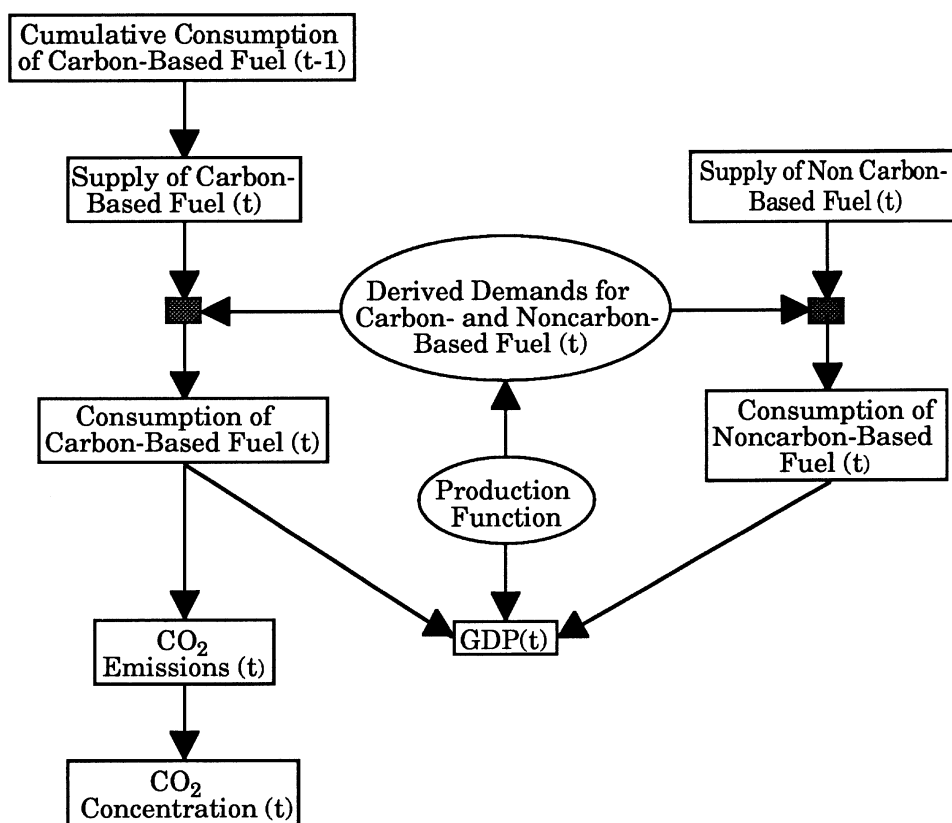


Figure 1. Schematic representation of the energy side of the emissions model.

recognize the model as the union of the original Nordhaus-Yohe (1983) probabilistic global-emissions model with the more recent (Nordhaus, 1994) DICE model. A detailed description of its highly aggregated structure can be found in Yohe and Wallace (1996), so it is sufficient for present purposes to highlight some of the properties that are most germane to this application.

Figure 1 schematically displays the energy side of the model structure. It shows that the demand sides of the simulated markets for carbon-based and noncarbon-based fuel in any year are derived directly and consistently from the production function that relates energy consumption, labor employment and the capital stock to gross domestic product in year  $t$ ,  $GDP(t)$ . The supply side for carbon-based fuel depends upon the depletion of carbon-based resources; it therefore depends upon cumulative consumption through the previous year. The supply side for noncarbon-based fuel depends upon historical trends and technological change. Both sides of the two markets interact in the two shaded boxes to determine contemporaneous levels of consumption – levels that feed back into the production function to determine the level of aggregate economic activity in year  $t$ . The consumption of

carbon-based fuel also determines the level of CO<sub>2</sub> emission, and that in turn works to determine CO<sub>2</sub> concentration.

The scale of the initial Monte Carlo simulation of alternative emissions scenarios is defined by nine uncertain parameters that include standard productivity and population-growth parameters, as well as unique unconstrained combinations of elasticities of substitution between energy and other productive inputs and between carbon-based and non-carbon based fuels. For each uncertain quantity, high, middle and low values are chosen so that they can reasonably be assigned subjective probabilities of 0.25, 0.50 and 0.25, respectively. Subsequent simulation focuses attention on the four parameters that contribute most to the range of estimates of emissions to 2100. An exhaustive, probabilistically weighted sampling across these four parameters adequately reflects the initial Monte Carlo outcomes of 1000 randomly selected scenarios drawn from the larger set of 3<sup>9</sup> (= 19, 683) possible combinations.

The resulting 81 (3<sup>4</sup>) scenarios are ranked in order of CO<sub>2</sub> emission in the year 2100 and are partitioned into seven groups. Following the methodology for selecting 'interesting' (i.e., representative) scenarios described by Yohe (1991), the groups are defined and representative scenarios are selected in a way that minimizes the probabilistically weighted sum of the squared errors involved in describing the entire distribution in emission for the year 2100 by the smaller collection of only seven trajectories. The likelihood value assigned to each trajectory represents the sum of the subjective weights of all the scenarios located in each specific group. CO<sub>2</sub> emission trajectories for the seven representative scenarios are depicted in Figure 2.

Since the representative scenarios emerge from a process that artificially collapses the content of 3<sup>9</sup> runs from one specific model into a manageable set of scenarios deemed representative and 'interesting', it is appropriate to question the degree to which they reflect anything more than the idiosyncrasies of the model, the selection process, or both. It is, however, comforting to note that the seven representative scenarios chosen reflect the diversity of current expert opinion reasonably well. The middle portion of their range, for example, spans completely the carbon emissions recorded by the IPCC in its six specified scenarios (see Houghton et al., 1992); indeed, approximately 20% of the likelihood range captured by the seven representative scenarios exceeds the highest IPCC emission trajectory (IS92e). The seven representative scenarios also lie between the 10th and 90th percentile results produced by Nordhaus (judged from Table 7.3 in Nordhaus, 1994), but showed much more potential on the high side of even the most recent 'modeler's choice' sample from Weyant (1996). Comparison with even a full set of alternative scenarios would not constitute validation of these scenarios. There is, nonetheless, some convincing evidence that the seven scenarios do, indeed, adequately cover the range of current opinion about what the future might hold and that their underlying structure does not produce anomalous cost or concentration statistics.

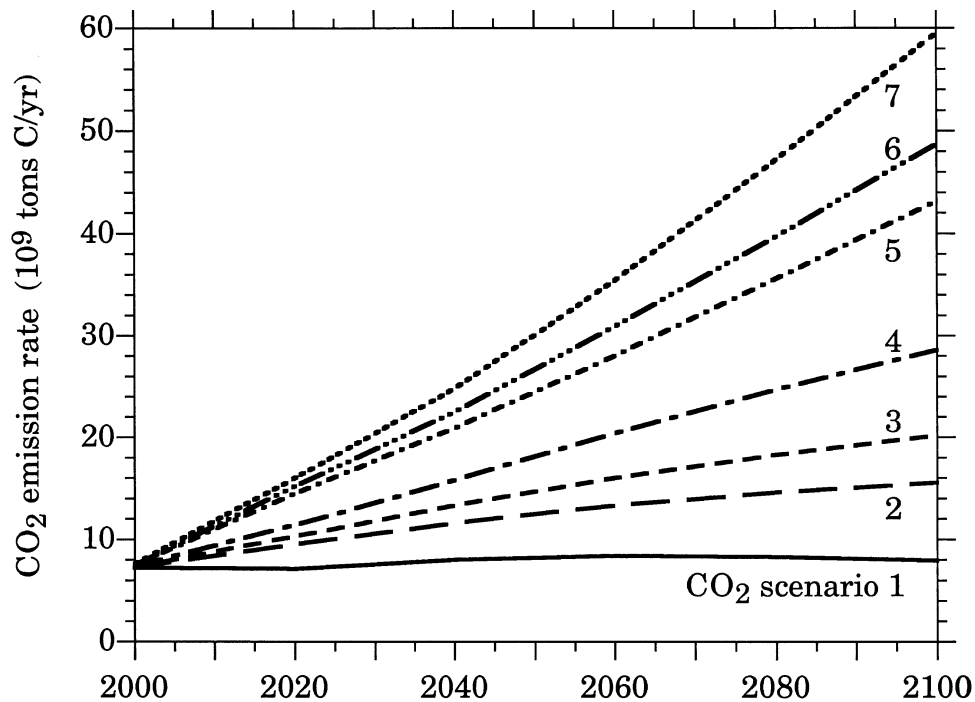


Figure 2. CO<sub>2</sub> emission trajectories from 2000 to 2100 for the seven representative scenarios.

The link between the CO<sub>2</sub> emission at time  $t$ ,  $E_{\text{CO}_2}(t)$ , and the contemporaneous atmospheric concentration of carbon dioxide,  $\text{CO}_2(t)$ , is drawn from the single-equation representation offered by Nordhaus in his DICE formulation (Equation (3.4) on page 26 of Nordhaus, 1994):

$$\text{CO}_2(t+1) = \beta E_{\text{CO}_2}(t) + (1 - \delta)\text{CO}_2(t), \quad (2.1)$$

where  $\beta$  and  $\delta$  are parameters to be estimated from the historical record. Given an assumed turnover time for the deep oceans of 120 years, Nordhaus reports that  $\delta = 0.00833 \text{ yr}^{-1}$  gave a 'best estimate' for  $\beta$  of 0.64. These are the middle values taken by Nordhaus (1994), and they are adopted here. There are, of course, other simple models that take emissions to concentrations and which reflect the potential that their parameterization might change over time. The DICE representation was chosen for convenience, but Yohe and Wallace (1996) indicate that the range of concentrations that emerge from the simulations again easily span the ranges of modelers' runs reported in Weyant (1996) for EMF-14. Therefore, taking advantage of convenience in this case is not very expensive.

The contributions of other greenhouse gases (GHGs) are handled by calculating equivalent-carbon-dioxide concentrations (ECD) – the amount of CO<sub>2</sub> which gives

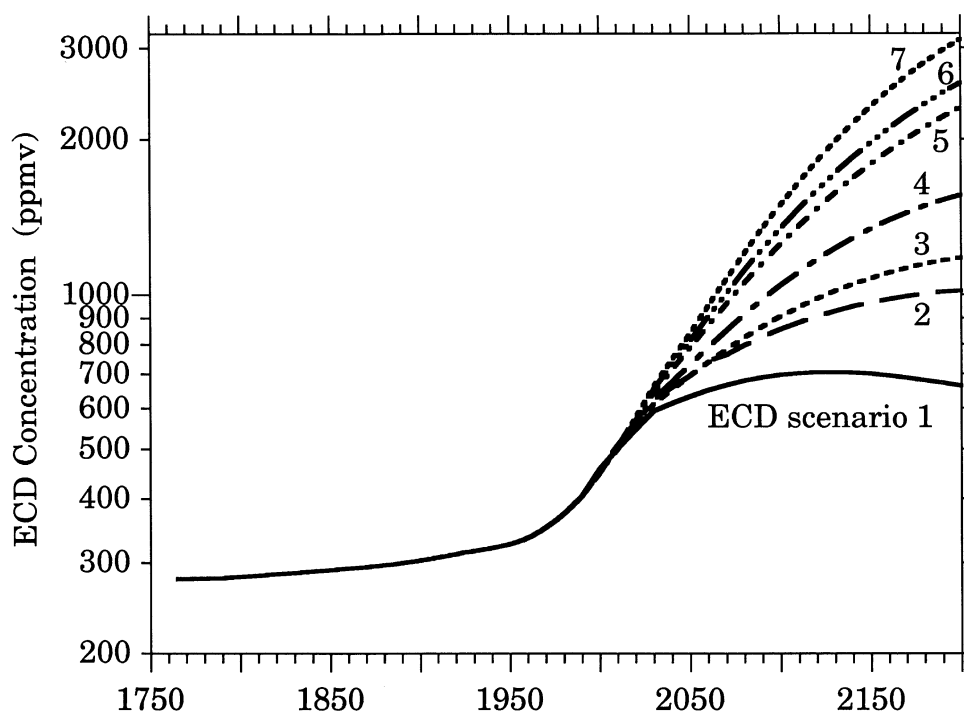


Figure 3. ECD concentration trajectories from 1765 to 2100 for the seven CO<sub>2</sub> emission trajectories of Figure 2.

the same radiative forcing as the radiative forcing by all *GHGs* (CO<sub>2</sub>, methane, nitrous oxide and the chlorofluorocarbons) – according to

$$ECD_i(t) = \begin{cases} ECD_{\text{obs}}(t), & 1765 \leq t \leq 1990 \\ \text{CO}_2(t)[1 + \alpha_i], & t > 1990, \end{cases} \quad (2.2)$$

where  $ECD_{\text{obs}}(t)$  is the observed equivalent-carbon-dioxide concentration in year  $t$  given by Shine et al. (1990) – which is slightly smaller (<4.8%) than that based on the most recent IPCC report (Houghton et al., 1996), principally due to the absence of the increase in tropospheric ozone – and the  $\alpha_i$  are estimated by applying an association between the forcing of other greenhouse gases and the annual growth rate of global *GDP* that is supported by the IPCC IS92 scenarios (Houghton et al., 1992). Applying this statistical association to the seven representative scenarios produces  $(\alpha_i, \text{GDP growth-rate})$  pairs of (0.390, 1.5%), (0.390, 1.5%), (0.334, 2.2%), (0.326, 2.3%), (0.286, 2.8%), (0.286, 2.8%), and (0.278, 2.9%) for scenarios 1 through 7, respectively. Figure 3 displays the resulting *ECD* concentration trajectories.

Three alternative sulfate-emission trajectories are examined for each *ECD* scenario. A base-case trajectory (*M*) is defined by:

$$E_{\text{SO}_2}^M(t) = \begin{cases} E_{\text{SO}_2, \text{obs}}(t), & 1856 \leq t \leq 1990 \\ E_{\text{SO}_2, \text{obs}}(1990) \left[ \frac{\text{CBF}(t)}{\text{CBF}_{\text{obs}}(1990)} \right]^\gamma, & t > 1990 \end{cases} \quad (2.3a)$$

where  $E_{\text{SO}_2, \text{obs}}(t)$  is the anthropogenic emission rate of sulfur in the form of  $\text{SO}_2$  given by Schlesinger et al. (1992),  $\text{CBF}_{\text{obs}}(1990)$  represents the carbon-based fuel consumption in 1990,  $\text{CBF}(t)$  represents the carbon-based fuel consumption projected along each carbon-emission scenario after 1990, and  $\gamma$  is the elasticity of sulfate emission with respect to the consumption of carbon-based fuel. The elasticity parameter  $\gamma$  is taken to be 0.7 for the *M* trajectory – a value roughly consistent with the U.S. experience since the passage of the Clean Air Act of 1977. A low-sulfate trajectory (*L*) is derived from the *M* trajectory by assuming a 1% cumulative annual decline against the base case,

$$E_{\text{SO}_2}^L(t) = \begin{cases} E_{\text{SO}_2, \text{obs}}(t), & 1856 \leq t \leq 1990 \\ (0.99)^{t-1990} E_{\text{SO}_2}^M(t), & t > 1990. \end{cases} \quad (2.3b)$$

This trajectory is designed to reflect active sulfate-emission-reduction policies being implemented sequentially across the globe. Finally, a high-sulfate trajectory (*H*) is defined by:

$$E_{\text{SO}_2}^H(t) = \begin{cases} E_{\text{SO}_2, \text{obs}}(t), & 1856 \leq t \leq 1990 \\ E_{\text{SO}_2, \text{obs}}(1990) \left[ \frac{\text{GDP}(t)}{\text{GDP}_{\text{obs}}(1990)} \right]^\eta, & t > 1990 \end{cases} \quad (2.3c)$$

where  $\text{GDP}_{\text{obs}}(1990)$  represents world-aggregate economic output in 1990,  $\text{GDP}(t)$  represents the sum of the value of goods and services projected to be produced across the globe along each emission scenario after 1990, and  $\eta$  is the elasticity of sulfate emission with respect to *GDP*, taken to be 0.8 – a value consistent with the U.S. experience since the 1950s. Trajectory *H* therefore includes the partial effects of emission-reduction policies with existing technology, but it does not presume that their adoption would be ubiquitous. Figure 4 displays the three alternative sulfate trajectories associated with *ECD* scenarios 1, 4, and 7.

Taken together, these sulfate emission trajectories roughly span the range reported to EMF-14 (Weyant, 1996) – a range that shows high, median and low emission for 2100 roughly equal to 3.5, 2 and 0.5 times 1990 levels, respectively. Those reported trajectories were not employed here, however, because they would not necessarily be consistent with the underlying economic activity of energy consumption patterns that spawned our carbon emissions. The three alternatives were created with an eye toward offering three qualitatively different, but possible, aggregate portraits of how future sulfate emissions might evolve. To that end, the middle case relates sulfate emissions to fossil-fuel consumption to reflect their sensitivity



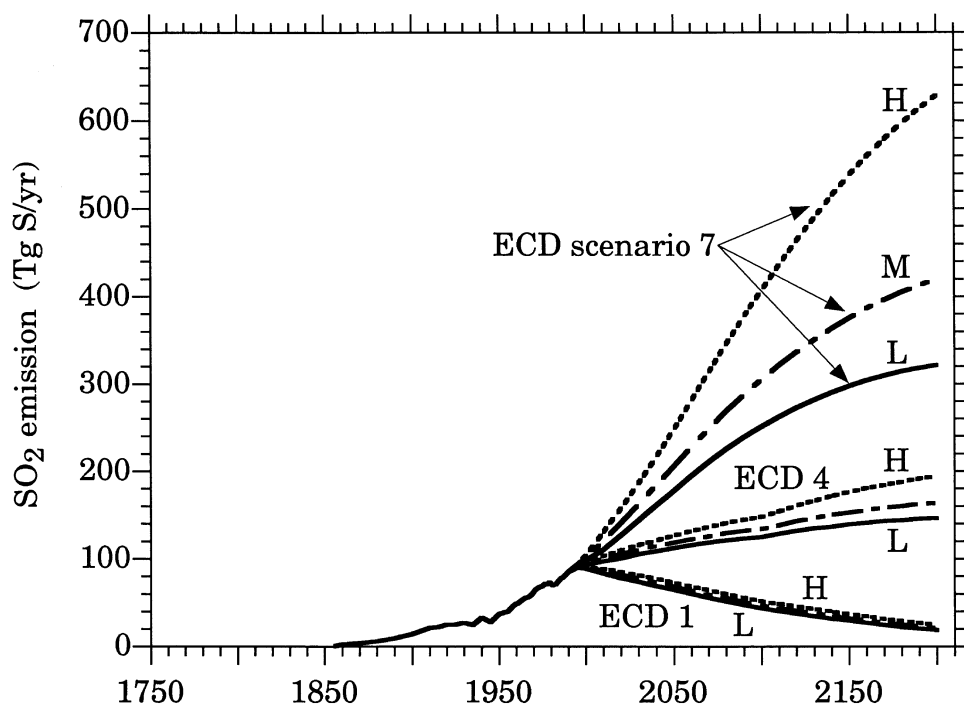


Figure 4. The low (*L*), medium (*M*) and high (*H*) alternative sulfate trajectories associated with ECD scenarios 1, 4, and 7.

to economic activity supported by increased energy efficiency and moderate effluent control; the U.S. experience under the Clean Air Act of 1977 was taken to be representative of both. The low scenario envisioned strenuous effluent control, and so it worked to reduce emissions directly from the middle case. The high scenario was meant to reflect the future when emerging high-energy consumers do little or nothing either to conserve energy or to control effluent. Emissions were therefore tied directly to *GDP*, and the U.S. experience prior to the Clear Air Act of 1977 was the representative guide.

## 2.2. TEMPERATURE AND SEA-LEVEL CHANGES

To calculate the change of temperature and the sea-level rise due to oceanic thermal expansion in response to the combined forcing by *GHGs* and *ASA*, we use an energy-balance-climate/upwelling-diffusion-ocean (*EBC/UDO*) model. The original, global version of this model was developed by Schlesinger, based on the model's original formulation by Hoffert et al. (1980), and was used by Schlesinger and colleagues to simulate the global-mean temperature evolution for the different *GHG* scenarios of the IPCC 1990 report (Bretherton et al., 1990), and for greenhouse policy studies (Schlesinger and Jiang, 1991; Hammitt et al., 1992; Schlesinger, 1993;

Lempert et al., 1994, 1996). The hemispheric version of the model was developed to study the influence on the climate system of ASA (Schlesinger et al., 1992) and putative solar-irradiance variations (Schlesinger and Ramankutty, 1992), and has been used to discover a 65–70 year oscillation in observed surface temperatures for the North Atlantic Ocean and its bordering continental regions (Schlesinger and Ramankutty, 1994a,b, 1995).

A hemispheric version of the model that explicitly calculates the individual temperature changes over land and ocean in each hemisphere (Ramankutty, 1994) has been used to investigate the influence on climate of volcanoes (Ramankutty, 1994) and the sun (M. E. Schlesinger, N. G. Andronova, and N. Ramankutty, in preparation), and to estimate the sensitivity of the climate system and the magnitude of the ASA forcing (N. G. Andronova and M. E. Schlesinger, in preparation). We use this hemispheric version of the model in the present study.

The model determines the changes in the temperatures of the atmosphere and ocean, the latter as a function of depth from the surface to the ocean floor. In the model the ocean is subdivided vertically into 40 layers, with the uppermost being the mixed layer and the deeper layers each being 100 m thick. Also, the ocean is subdivided horizontally into a polar region where bottom water is formed, and a nonpolar region where there is upwelling. In the nonpolar region, heat is transported upwards toward the surface by the water upwelling there and downwards by physical processes whose effects are treated as an equivalent diffusion. Heat is also removed from the mixed layer in the nonpolar region by a transport to the polar region and downwelling toward the bottom, this heat being ultimately transported upward from the ocean floor in the nonpolar region. The atmosphere in each hemisphere is subdivided into the atmosphere over the ocean and the atmosphere over land, with heat exchange between them.

In addition to the radiative forcing, ten principal quantities must be prescribed in the model: the temperature sensitivity of the climate system,  $\Delta T_{2\times}$  – the equilibrium surface-air temperature change in response to the radiative forcing equivalent to a doubling of the CO<sub>2</sub> concentration,  $\Delta F_{2\times}$  (4.39 Wm<sup>-2</sup>); the vertically uniform upwelling velocity for the global ocean,  $W$  (4 m/yr); the vertically uniform thermal diffusivity,  $\kappa$  (0.63 cm<sup>2</sup> s<sup>-1</sup>), by which all non-advective vertical heat transport in the ocean is parameterized; the depth of the oceanic mixed layer,  $h$  (70 m); the warming of the polar ocean relative to the warming of the nonpolar ocean,  $\Pi$  (0.4); the air-sea and air-land heat exchange coefficients,  $\lambda_{a,o}$  (49 Wm<sup>-2</sup>/°C) and  $\lambda_{a,L}$ ; the interhemispheric heat transfer coefficients for the atmosphere and ocean,  $\beta_a$  (3.39 Wm<sup>-2</sup>/°C) and  $\beta_o$  (3.07 Wm<sup>-2</sup>/°C); and the heat exchange coefficient between the atmosphere over land and ocean,  $k$ . Here we use our usual values for  $W$ ,  $\kappa$ ,  $h$ ,  $\Pi$ ,  $\lambda_{a,o}$ ,  $\beta_a$  and  $\beta_o$  (Schlesinger et al., 1992);  $\lambda_{a,L} = \infty$  and  $k = 2.5$  Wm<sup>-2</sup>/°C; and choose  $\Delta T_{2\times}$  to be either 1.5 °C, 2.5 °C or 4.5 °C.

The hemispheric radiative forcing in the model is

$$\Delta F_h(t) = \Delta F_{2\times} \frac{\ln[ECD(t)/ECD(1765)]}{\ln 2} + \alpha_h \Delta F_{ASA}(1978) \frac{E_{SO_2}(t)}{E_{SO_2}(1978)}, \quad (2.4)$$

where  $ECD(t)$  is the equivalent-carbon-dioxide concentration given by Equation (2.2) and  $ECD(1765) = 279$  ppmv;  $E_{SO_2}(t)$  is the sulfate emission given by Equation (2.3);  $\Delta F_{ASA}(1978)$  is the radiative forcing of ASA in 1978 (the year for which Charlson et al. (1991) made the first radiative-transfer calculation for the clear-atmosphere component thereof), with the value here taken to be either 0,  $-0.6$  or  $-1.2$   $W\ m^{-2}$ ; and  $\alpha_h$  is 1.6 for the northern hemisphere and 0.4 for the southern hemisphere, such that 80% of the global ASA forcing occurs in the northern hemisphere and 20% in the southern hemisphere. The change in global-mean surface temperature is shown in Figure 5.

The model calculates the change in sea level due to thermal expansion, changes in small glaciers, and changes in the Greenland and Antarctic ice sheets. The sea-level change due to thermal expansion is given by

$$\Delta SL_{TE}(t) = \sum_{l=1}^{40} \frac{[\rho(p_l, T_l) - \rho(p_l, T_l + \Delta T_l(t))]\Delta z_l}{\rho(p_l, T_l + \Delta T_l(t))}, \quad (2.5)$$

where  $l$  denotes the vertical layers in the ocean,  $\rho(p_l, T_l)$  is the density of sea water at pressure  $p_l$  and undisturbed reference temperature  $T_l$ , and  $\rho(p_l, T_l + \Delta T_l(t))$  is the corresponding density at disturbed temperature  $T_l + \Delta T_l(t)$ , with  $\Delta T_l(t)$  the global-mean temperature change calculated by the *EBC/UDO* model for ocean layer  $l$  at time  $t$ .

We calculate the change in sea level contributed by the Greenland ice sheet, the Antarctic ice sheet and small glaciers following Wigley and Raper (1993),

$$\frac{dz_G}{dt} = 1.5\beta_G\Delta T(t), \quad (2.6)$$

$$\frac{dz_a}{dt} = \beta_A\Delta T(t), \quad (2.7)$$

$$\frac{dz_{sg}}{dt} = \begin{cases} \frac{-z_{sg} + (Z_o - z_{sg})\beta\Delta T}{\tau}, & \text{for } 0 \leq z_{sg} < Z_o \\ 0, & \text{for } z_{sg} = Z_o, \end{cases} \quad (2.8)$$

where  $z_G$  is the change in sea level due to the Greenland ice sheet, with  $z_G(1765) = 0$ ,  $\beta_G = 3 \times 10^{-4}$   $m\ yr^{-1}/^\circ C$ ,  $\Delta T(t)$  the change in the global-mean atmospheric temperature since 1765, and the factor 1.5 accounts for the poleward amplification of the temperature change in the northern hemisphere;  $z_A$  is the change in sea level due to the Antarctic ice sheet, with  $z_A(1765) = 0$  and  $\beta_A = -2 \times 10^{-4}$   $m\ yr^{-1}/^\circ C$ ; and  $z_{sg}$  is the change in sea level due to the melting of small glaciers,

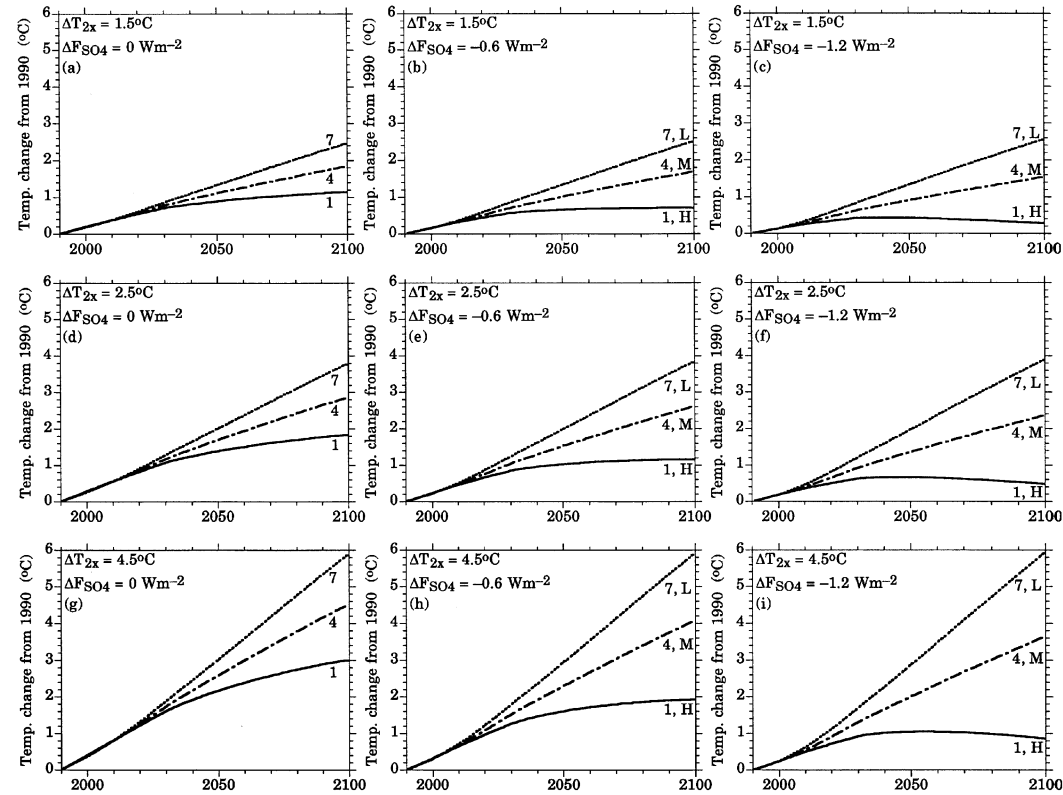


Figure 5. Change in global-mean surface temperature from 1990 for three pairs of *ECD* scenario and sulfate trajectory, (1, *H*), (4, *M*) and (7, *L*) that span the range of results, each for three alternate sulfate forcing values,  $\Delta F_{\text{SO}_4} = 0, -0.6$  and  $-1.2 \text{ Wm}^{-2}$ , and three climate sensitivities,  $\Delta T_{2x} = 1.5, 2.5$  and  $4.5 \text{ }^\circ\text{C}$ .

with  $z_{sg}(1765) = 0$ ,  $Z_o = 0.5$  meters,  $\beta = 0.25/^\circ\text{C}$  and  $\tau = 20$  years. The change in sea level, shown in Figure 6, ranges in 2100 from 10.8 cm for the smallest climate sensitivity and highest sulfate ( $\Delta T_{2\times} = 1.5^\circ\text{C}$  and scenario 1H with  $\Delta F_{ASA}(1978) = -1.2 \text{ Wm}^{-2}$ ) to 89.4 cm for the highest climate sensitivity and lowest sulfate ( $\Delta T_{2\times} = 4.5^\circ\text{C}$  and Scenario 7 with  $\Delta F_{ASA}(1978) = 0 \text{ Wm}^{-2}$ ). Our maximum is virtually identical to that of the most recent IPCC report (Warrick et al., 1996), while our minimum is about 50% smaller.

### 2.3. SEA-LEVEL-RISE TRAJECTORIES TO ECONOMIC COST

We calculate the economic damage that might be attributed to future sea-level rise in the absence of any decision to protect threatened property in terms of the value of that property at the (future) time of inundation, taking into account any adaptation that might have occurred naturally and efficiently prior to flooding and abandonment. Adaptation, here, means any sort of cost-reducing activity undertaken in response to the threat of future (or immediate) inundation. Some adaptation occurs ‘naturally’ as, for example, markets’ incorporating the threat. Other adaptation requires specific action by specific individuals – such as deciding to protect a particular piece of property. Some adaptation is efficient, in the sense of minimizing cost; other adaptation may be ‘second best’, but it still lowers cost and improves welfare. Meanwhile, protection can, here, involve building dikes, building seawalls, nourishing beaches, raising houses – any activity that prevents (or reduces the likelihood of) damage from rising seas. The strategy chosen is the one that achieves the objective at least cost. Portraits of both future economic development and efficient market adaptation are therefore required.

The model employed here produces those portraits for square cells of developed coastal property (500 m by 500 m) that span the coastlines of locations chosen for inclusion in the United States sample. Satisfactory descriptions of how future development might affect real-estate values in each coastal cell are derived from empirical market analyses of how property values might change as functions of ‘driving socio-economic variables’ like population and real income. Abraham and Hendershott (1993), for example, explain the current rate of change in property values in terms of a lagged rate of change, the rate of growth of (local) population, and the rate of growth of real per capita *GDP*. Historically based portraits of the appreciation of the real-property value are produced by inserting into accessible empirical studies such as Abraham and Hendershott (1993), scenarios of how ‘driving socio-economic variables’ might move as the future unfolds. Applied with care in the absence of any anticipated, fundamental structural change in the real-estate marketplace, the resulting development trajectories offer portraits of the evolving context of the sea-level-rise problem. Matching the driving variables of property appreciation with their antecedents in the economic-activity model brings an additional degree of consistency to bear on the analysis. Yohe et al. (1996) outline the procedure in more detail and highlight the sources of data.

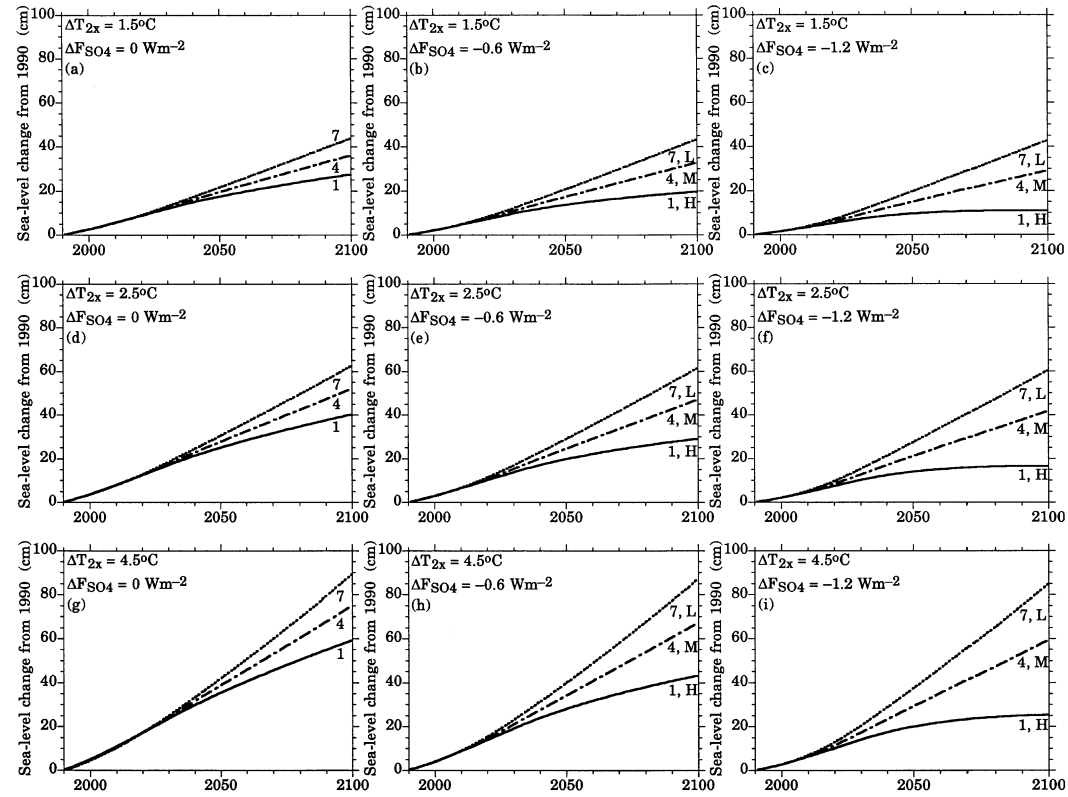


Figure 6. Change in sea level from 1990 for three pairs of ECD scenario and sulfate trajectory, (1, H), (4, M) and (7, L), that span the range of results, each for three alternate sulfate forcing values,  $\Delta F_{\text{SO}_4} = 0, -0.6$  and  $-1.2 \text{ Wm}^{-2}$ , and three climate sensitivities,  $\Delta T_{2x} = 1.5, 2.5$  and  $4.5^\circ\text{C}$ .

Satisfactory descriptions of how real-estate markets might respond on a more micro, local level in the face of threatened inundation from rising seas are more difficult to create. Yohe (1989) and Yohe et al. (1996) provide some insight into how to proceed. By 1996 it had become widely accepted that land and structures should be considered separately. Procedures that would account appropriately for the economic cost of losing one would not necessarily account accurately for the economic cost of losing the other. In particular, the value of the land lost to rising seas should, in most cases, be estimated on the basis of the value of land located far inland from the ocean. It is therefore assumed here implicitly that any price gradient which placed higher values on parcels of land in direct correlation with their proximity to the ocean would, in a very real sense, simply migrate inland as shoreline property disappeared under rising seas. Ignoring what could be significant transfers of wealth for the purpose of computing social cost, as is the convention of cost-benefit analysis, the true economic cost of inundation can thus be captured in most cases by the value of the land that was, in an economic sense, actually lost – interior land equal in area to the abandoned and inundated property. The exception to this procedure occurs when rising seas threatened a barrier island where the property-value gradients encroached from two sides. It is still possible to use the value of interior land to reflect costs, but care must be taken to note when interior values begin to reflect the higher values defined as both gradients converged on the middle of the island. Yohe (1989) provides a description of how this case is accomplished.

The economic value of structures can meanwhile be assumed to depreciate over time as the threat of impending inundation and abandonment became known. Structures would be lost at the moment of inundation, to be sure, but their true economic value at that point could be zero with perfect foresight and enough advanced warning. Despite stories of individuals' reluctance to abandon threatened property in, for example, flood plains, the results of investigations into how markets react to low probability-high cost events strongly support the assertion that the market-value of structures does indeed decline over time in response to the pending cost of a growing threat. For example, MacDonald et al. (1987) examined homeowner behavior in the face of the threat of flooding and found some degree of aggregate response. Brookshire et al. (1985) had previously found similar response to earthquakes even when individuals passed on the opportunity to purchase insurance. All of this work offers evidence to suggest that market values should process information offered by experts about low-probability natural hazards. The assumption made in support of this work is that property values should, over the long term, and in the face of gradual manifestations of rising seas, internalize the threat, particularly given some increased validation of the information being offered by the expert community.

Ill-timed or incomplete (uncertain) abandonment, caused by uncertainty about the rate of future sea-level rise and/or a disbelief that existing property would actually be abandoned, might undercut maximum efficiency because either source of imperfect information would support only an incomplete reaction to the threat

of rising seas. The value of lost structures under these conditions would then not be zero; it would, instead, equal the remaining value of (shoreline) structure at the time of inundation. The worst case of imperfect information and uncertain abandonment would allow absolutely no market adaptation and thus no time for any structural depreciation at all – a situation that would perhaps be the result of a sudden realization that a policy of abandonment would, indeed, be followed. Regardless of its cause, this worst-case scenario is modeled to capture circumstances under which the cost attributed to inundation by rising seas would be as large as possible. Storms, of course, raise the possibility of multiple losses on the same site and could, therefore, exaggerate even these worst-case estimates.

Armed with these accounting conventions, we divide the planning of how to respond to rising seas along a developed coastline into two distinct decisions that are modeled as efforts to maximize discounted intertemporal welfare (i.e., the net benefits of any protection strategy minus the cost of its implementation). The first, a decision to protect the coastline starting at some time  $t_o$ , is thought to be reversible; more specifically, it is assumed that it would always be possible to decide at some later time  $T$  to abandon property that had previously been protected. The alternative decision not to protect shoreline property (or to stop protection at time  $T$ ), is taken to be irreversible. Planning any heroic and expensive attempt to reclaim previously abandoned property is, ultimately, assumed to be dominated in every case by the less-expensive option of protecting (or continuing to protect) that property all along.

The (net) benefit side of a decision to protect a shoreline from time  $t_o$  through time  $T$  is modeled as the true opportunity cost of abandoning coastal property, and calculation of that opportunity cost requires a time trajectory of the (future) value of property vulnerable to sea-level rise along some specific scenario. Let  $p(t)$  represent the time trajectory of property values that would be lost at time  $t$  if it were not somehow protected. Assuming the efficiency of perfect foresight and associated market-based adaptation,  $p(t)$  should reflect only the value of parcels of interior land equal in area to inundated shoreline property. Efficiency conditions need not be satisfied in every case, though. Protection decisions may, indeed, incorporate suboptimal decisions based on admittedly imperfect information and incomplete adaptation. In such a case,  $p(t)$  would include not only the value of interior land, but also some proportion of the value of threatened structures. If there were absolutely no foresight, in fact,  $p(t)$  would include 100% of the value of coastline structures. In any case,  $p(t)$  is not a cumulative statistic; it is, quite simply, the value of (unprotected) property that would be lost at time  $t$ .

Turning now to a generic representation of the present value of the net benefit to society from its protecting property from time  $t_o$  through time  $T$ , let  $\rho(t)$  represent the time trajectory of appropriate property values (per unit area) and  $A(t)$  represent the incremental area of land threatened at time  $t$ . The  $\rho(t)$  series notationally reflects all of the complication caused by appreciation and adaptation that is outlined above,



while the  $A(t)$  series reflects an inundation trajectory. In this case,  $p(t) = \rho(t)A(t)$ , and the present value of net benefits is:

$$PV[B(t_o, T)] = \int_{t_o}^T p(t)e^{-rt} dt - e^{-rT} \rho(T) \int_0^T A(t) dt. \quad (2.9)$$

The first term in Equation (2.9) represents the value of protection, expressed in terms of the sum of the value of property that was not lost from time  $t_o$  through time  $T$ . The second term represents the value of all of the property that had been protected but was subsequently abandoned at time  $T$ . All of this abandoned property is valued by  $\rho(t)$  from  $t_o$  through  $T$ , the time of abandonment, but its ultimate loss is fully discounted back to the present ( $t = 0$ ). This structure allows property to be protected for a finite period of time. That is, a decision to protect at  $t_o$  does not commit anyone to protect indefinitely; protection will continue only so long as its benefits outweigh its costs.

The cost of protection from time  $t_o$  through time  $T$  is easier to frame. Let  $c(t)$  represent the time trajectory of protection costs along the same specified sea-level-rise scenario. The present value of those costs is then, simply

$$PV[C(t_o, T)] = \int_{t_o}^T c(t)e^{-rt} dt. \quad (2.10)$$

Given Equations (2.9) and (2.10), even in their most general form, the planning problem is quickly reduced to one of picking the pair  $(t_o^*, T^*)$  that maximizes the present value of the net benefit of protection:

$$PV[B(t_o, T)] - PV[C(t_o, T)], \quad (2.11)$$

with  $t_o^* < T^*$  imposed on the solution by the irreversibility of the decision to abandon.

Taken to its practical level, the benefit-cost planning criterion embodied in Equation (2.11) is applied to each cell that was threatened by inundation at any time  $t_o$  along every sea-level-rise trajectory. If the net benefit of protection turns out to be positive for any threatened cell, then we record the stream of protection costs (fixed investment at time  $t_o$  and variable costs through time  $T$ ). If the net benefit of protection is negative, however, then the cell is abandoned and we register the (undiscounted) second term of  $PV[B(t_o, T)]$  as a cost. Summed over all of the cells in the sample, these cost series produce estimates of actual economic cost for the United States in decadal increments; and so they can be used to produce not only estimates of transient costs over time, but also discounted costs through the year 2100.

### 3. Analysis, Procedures and Results

The seven representative CO<sub>2</sub>-emission trajectories drawn from the global economic-energy model described in Section 2.1, expanded to include forcing by other greenhouse gases and associated sulfate emissions, support probabilistically weighted

portraits of how the future might unfold. Each is run with three different climate sensitivities,  $\Delta T_{2\times}$ , that feed associated damage estimates back into the model of underlying economic activity, and with three distinct but associated sulfate emissions trajectories, each permuted across three distinct values for the sulfate forcing parameter,  $\Delta F_{ASA}$  (1978). Each representative emissions trajectory therefore supports 36 alternative futures for a total of 252 scenarios. A fourth set of scenarios is also produced for each representative emissions trajectory by essentially ignoring sulfate forcing, and sampling over the full range of climate sensitivities, thereby generating another 28 alternative futures. We run the resulting total of 280 scenarios through the *EBC/UDO* model to produce 280 different sea-level-rise trajectories to which the costing model is applied. Costs are computed along each sea-level trajectory on a cell-by-cell basis for thirty sample sites, and the results are aggregated to produce estimates of total annual cost for the United States in decadal increments from the year 2000 through the year 2100. The sites, identified explicitly in Yohe (1989) and Yohe et al. (1996), were selected systematically from around the coastline and have been judged to be reasonably representative – at least sufficiently representative to support aggregate estimates of cost. Six different cost-of-protection assumptions are employed in each case, and ranges of property value appreciation are employed that were consistent with the levels of economic activity associated with the underlying and corresponding emissions paths.

Simulation over the complete set of alternative trajectories thereby produces initial time series estimates of the anticipated cost of sea-level rise across a wide range of possible futures; each is indexed by its associated anticipated level of sea-level rise through the year 2100 (denoted by  $S$  in the following discussion). These time series subsequently support a two-stage procedure for estimating a relationship that explained the variation in costs in any year  $t$ ,  $C[t; S, P, V(t)]$ , by tracking the variations in  $S$ , the real protection cost,  $P$  (indexed such that \$750 per linear foot for protection against a one meter sea-level rise was unity), and the real value of property at the time of possible abandonment,  $V(t)$  (indexed such that the 1990 value was unity). More specifically, the first stage assumes a relationship of the form:

$$C[t; S, P, V(t)] = e^{A(t)} S^{a(t)} P^{\beta(t)} V(t)^{\gamma(t)} \quad (3.1)$$

for each decadal anniversary from the year 2000 through the year 2100. The  $A(t)$  parameter in these estimate functions is an initializing scale parameter, while  $a(t)$ ,  $\beta(t)$  and  $\gamma(t)$  all serve functionally as elasticities; i.e., the last three terms indicated the sensitivity of total cost, measured in percentage terms, to percentage changes in  $S$ ,  $P$  and  $V(t)$ , respectively.

Second-stage estimates exploit an observed linear sensitivity of the initializing parameter  $A(t)$  to time and the time insensitivity of the elasticity estimates to produce a summary relationship of the form:

$$C[t; S, P, V(t)] = e^{A+\alpha t} S^a P^\beta V(t)^\gamma. \quad (3.2)$$

Table II  
 Transient costs with perfect foresight (millions 1990\$ per year)

Year	Anticipated sea-level rise through the year 2100 (cm)								
	10	20	30	40	50	60	70	80	90
2010	4.43	13.44	24.69	38.02	53.13	69.84	88.01	107.52	128.30
2020	5.51	15.59	28.64	44.10	61.63	81.01	102.09	124.73	148.83
2030	6.33	17.91	32.90	50.65	70.78	93.05	117.25	143.25	170.94
2040	7.16	20.25	37.20	57.27	80.03	105.20	132.57	161.97	193.27
2050	8.10	22.91	42.10	64.81	90.58	119.07	150.04	183.31	218.74
2060	9.07	25.66	47.13	72.56	101.41	133.31	167.99	205.24	244.91
2070	10.13	28.65	52.63	81.03	113.24	148.86	187.59	229.19	273.48
2080	11.33	32.03	58.85	90.60	126.62	166.45	209.75	256.26	305.79
2090	12.66	35.82	65.80	101.31	141.58	186.11	234.53	286.54	341.91
2100	14.16	40.05	73.57	113.27	158.30	208.09	262.23	320.38	382.29

Assuming perfect foresight, for example, this estimation procedure fits Equation (3.2) with

$$C[t; S, P, V(t)] = e^{-3.45+0.0113t} S^{1.5} P^{0.25} V(t)^{0.26}. \quad (3.3)$$

The first stage produces stable estimates with  $R^2$  values uniformly in excess of 0.95; the second stage  $R^2$  is 0.994. Without any foresight, by way of contrast,

$$C[t; S, P, V(t)] = e^{-3.85+0.014t} S^{1.6} P^{0.40} V(t)^{0.09}. \quad (3.4)$$

The correlation is a bit smaller in this case, but the second stage  $R^2$  is still 0.951. Notice that lost foresight brings an increased sensitivity of cost to both changes in anticipated sea-level rise through the year 2100 and to changes in the cost of protection, but a lower sensitivity to the appreciated value of property. It is conceivable, however, that some of the power of appreciating property values in explaining costs over time is captured in the higher time trend. It is clear, though, that protection plays a larger role in the foresight case, not only in defining appropriate responses to rising seas, but also in determining the expected cost of those responses.

Tables II and III record the annual transient cost schedules described by Equations (3.3) and (3.4) for decades beginning in 2010 and running through the year 2100 under the best-guess assumptions about property-value appreciation and the cost of protection. Figure 7 displays the Table III results graphically – transient costs in the absence of foresight. Each curve in Figure 7 portrays, in particular, the estimated annual cost attributable to sea-level rise either through abandonment of property or its protection as a function of total sea-level rise anticipated through the year 2100. If 50 cm in sea-level rise were anticipated through the turn of the next century, for example, then Table III and Figure 7 show that something on the order of \$61 million (1990\$), \$110 million, and \$222 million in cost could be expected

Table III  
 Transient costs without foresight (millions 1990\$ per year)

Year	Anticipated sea-level rise through the year 2100 (cm)								
	10	20	30	40	50	60	70	80	90
2010	4.59	14.02	26.94	42.81	61.31	82.23	105.39	130.67	157.95
2020	5.35	16.33	31.37	49.85	71.39	95.75	122.72	152.16	183.93
2030	6.21	18.95	36.40	57.84	82.85	111.11	142.41	176.57	213.44
2040	7.17	21.87	42.01	66.76	95.62	128.25	164.37	203.80	246.35
2050	8.27	25.25	48.51	77.08	110.40	148.07	189.78	235.30	284.43
2060	9.52	29.05	55.80	88.67	127.00	170.32	218.30	270.66	327.17
2070	10.94	33.38	64.12	101.90	145.95	195.74	250.87	311.05	375.99
2080	12.57	38.38	73.72	117.16	167.80	225.05	288.44	357.62	432.29
2090	14.46	44.13	84.76	134.70	192.93	258.74	331.63	411.17	497.03
2100	16.62	50.73	97.46	154.87	221.81	297.49	381.29	472.74	571.45

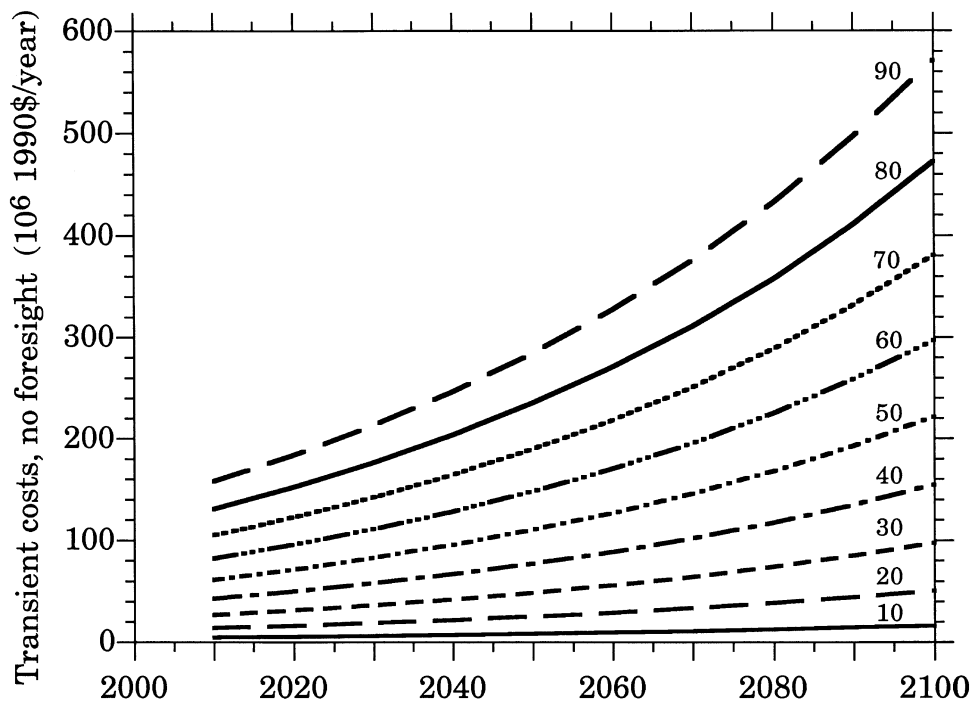


Figure 7. Transient costs in the absence of foresight from 2010 to 2100, indexed as a function of the anticipated sea-level rise (cm) through the year 2100.

in the years 2010, 2050 and 2100, respectively. Those costs should be expected to climb to \$158 million, \$284 million and \$571 million per year, respectively, if anticipated sea-level rise through 2100 were thought to be 90 cm instead of 50 cm.

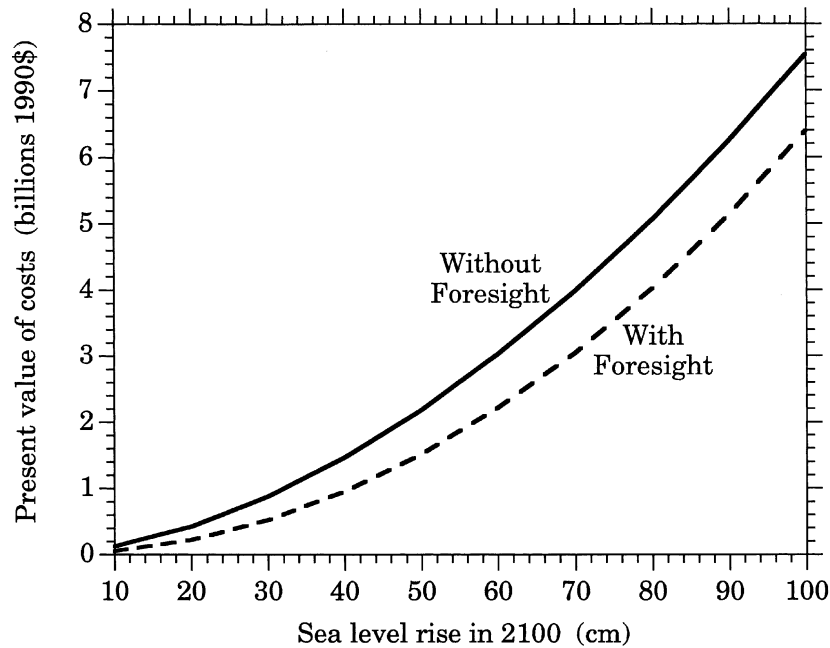


Figure 8. Present value of cost indexed as a function of anticipated sea-level rise through the year 2100, with and without foresight, calculated with a 3% discount rate.

The first-stage procedure also supports estimates of the present value of cost,  $PV[C(t; S, P, V(t))]$ , again indexed as a function of anticipated sea-level rise through the year 2100. With foresight and a 3% discount rate, in particular,

$$PV[C(t; S, P, V(t))] = e^{-4.3} S^{2.08} P^{0.27} V(t)^{0.26}, \quad (3.5)$$

while, without foresight,

$$PV[C(t; S, P, V(t))] = e^{-2.8} S^{1.79} P^{0.33} V(t)^{0.10}. \quad (3.6)$$

Figure 8 displays these schedules, again assuming best-guess values for protection expense and property appreciation. Notice that perfect information lowers cost, but perhaps not by as much as might be expected – by 40% if 50 cm worth of higher seas were anticipated by the year 2100, but only by slightly more than 15% if 100 cm in sea-level rise were thought to be most likely. The potential harm caused by rising seas climbs so smoothly that the absolute value of perfect adaptation with perfect information grows much more slowly than the total cost of inundation.

Equations (3.5) and (3.6) also support estimates of the expected present value of the cost attributable to sea-level rise across the probabilistically weighted emissions trajectories described in Section 2. The first section of Table IV shows results that ignore the potential effect of sulfate aerosols on radiative forcing, but include equally weighted assumptions about climate sensitivity across the 1.5 °C to 4.5 °C

Table IV

The expected present value of the cost of greenhouse-gas-induced sea-level rise on the developed U.S. coastline

Case	Expected present value (millions of 1990 dollars (1990\$) computed with a 3% discount rate)		
	10th percentile	Mean	90th percentile
	<i>No sulfate, 41 (10, 81)<sup>a</sup></i>		
Foresight	76	1326	3611
No foresight	147	1836	4620
	<i>Base-case sulfate, 35 (9, 69)</i>		
Foresight	52	949	2812
No foresight	112	1381	3715
	<i>Low sulfate, 40 (10, 75)</i>		
Foresight	73	1325	3590
No foresight	143	1768	4392
	<i>High sulfate, 25 (6, 56)</i>		
Foresight	21	525	1870
No foresight	53	784	2451

<sup>a</sup> Sea-level rise in 2100. Ninety percent confidence interval for sea-level rise through the year 2100 indicated in parentheses.

range advanced by the Intergovernmental Panel on Climate Change. With and without foresight, the expected present value is \$1.3 billion (1990\$) and \$1.8 billion (1990\$), respectively. Note, however, that these estimates are surrounded by enormous 90% confidence intervals that were determined by recognizing climatic uncertainty (reflected by 90% confidence bounds on anticipated sea-level rise through 2100) and estimation error; they do not, it must be emphasized, capture the potential effect of model uncertainty.

The potential effect of sulfate emissions on these estimates is also examined. Recall that three different sulfate trajectories are considered with three equally weighted assumed forcings. The first is a base-case sulfate trajectory (denoted *M* in Figure 4) defined by an elasticity of sulfate emissions with respect to the consumption of fossil fuel equal to 0.7. In this case, sulfate emission generally climbs from 1990 levels by 25% to 90% through the year 2100, and Table IV shows a 25% reduction in both the estimated expected value of costs and the extremes of the 90% confidence interval for anticipated sea-level rise through the year 2100. A low sulfate emission trajectory (*L*), defined by a 1% annual decline from the base case, is also considered. In this case, sulfate emission generally falls

from 1990 levels by 50 to 70% through the year 2100, and Table IV shows little effect on either the estimated expected value of costs or the range of anticipated sea-level rise compared to the case with no sulfate. Finally, a high trajectory ( $H$ ) is defined by an elasticity of sulfate emissions with respect to world  $GDP$  equal to 0.8. In this last case, sulfate emission generally climb by as much as 200%, and, not surprisingly, the expected discounted cost of sea-level rise falls by almost two-thirds in the mean and by 50% in the upper extreme, as anticipated sea-level rise through the year 2100 falls by more than 30% at the upper tail and by nearly 40% in its mean.

For purposes of comparison with the most recent estimates of sea-level rise, it is useful to note that the final cumulative probability distribution offered in Table 7-3 of Titus and Narayanan (1995) reports a median through 2100 of 34 cm surrounded by a 90% confidence interval bounded on the low and high sides by 5 cm and 77 cm, respectively. Table IV displays comparable statistics. The lower boundary of the confidence intervals ranges from 6 cm through 10 cm, depending upon assumptions about sulfate-emission trajectories, the higher boundaries are fixed between 56 cm and 81 cm, and the medians cover the range from 25 cm through 41 cm.

#### 4. Conclusion

The results recorded here accomplish the three tasks identified in the introduction. Reduced-form estimates of the transient cost of anticipated sea-level rise through the year 2100, with and without foresight, are provided by Equations (3.3) and (3.4). Both display nonlinearity in sea-level rise, but neither reaches the standard quadratic form frequently employed in the damage functions of integrated assessment models (see, e.g., Equation (2.10) in Nordhaus, 1994). Comparing the sea-level-rise elasticity estimates in Equations (3.5) and (3.6) with their counterparts in Equations (3.3) and (3.4) suggests, however, that this nonlinearity is amplified when present-value calculations are made across a wide range of probabilistically weighted futures – amplified across that range by nonlinearity in the relationship between greenhouse-gas concentrations and sea-level rise. Finally, Table IV notes that the best-guess estimates of the expected present value of cost are surrounded by large error bands that are very sensitive to changes in the way sulfate emissions are modeled. The specifics of the best-guess estimates continue to underscore the trend toward lower costs. Indeed, absent any consideration of sulfate emissions, amortized annual values consistent with the expected present values listed in Table IV are \$40 million (1990\$) and \$55 million with and without perfect foresight, respectively; add consideration of the base-case sulfate emissions, these annual values fall to \$28 million and \$40 million. Readers interested in considering these estimates in a broader context should, however, recognize that they, like the earlier estimates recorded in Table I, cover only developed property in the United States and that they ignore the effect of storms.

It should be noted, as well, that several methodological advances are embodied in this work. The marriage of three models (one emissions model, one simple climate/ocean model, and one economic impacts cum adaptation model) represents a modest advance in linking emissions, driven by representative views of the pace of economic activity, with a careful consideration of their downstream cost. Linkages of this sort are not always the next logical step in integrated assessment, but they are essential in contexts where internal consistency and unknown feedbacks between social and natural-science components are to be examined. It would not be enough, in this case for example, to simulate the sea-level rise model around, say, the IPCC IS92 emissions scenarios because property valuations and, as a result, downstream costs will be driven into the future by the same variables that will drive the aggregate economic activity that underlies those emissions. Nor would it be enough to run the sea-level rise model for a variety of arbitrarily selected sulfate scenarios (for the same reason, essentially). There are, in short, a multitude of internally inconsistent combinations of emissions/coastal-development scenarios that should not be studied; and if they are, the ‘insight’ that they suggest should not be believed.

Sea-level rise is, fortunately, a relatively easy arena within which to accomplish this sort of linkage, since the natural and economic impacts are essentially self-contained. Simulation across ranges of possible futures shows clearly that the sensitivity of natural and economic effects to underlying driving scenarios produces wide uncertainty in even a summary statistic like the present value of costs, even when consistent correlations of drivers and outcomes are allowed. Consistent modeling does, however, show that assuming different sulfate futures across the full range of aggregate economic possibilities can move the distribution of outcomes discernibly – much lower and tighter for high-sulfate trajectories.

The structure and the functional results reported here may, finally, be somewhat exportable to coastal areas where protection decisions will be made using cost-benefit criteria and where property markets are similarly structured. Differences in coastal topography may be important, to be sure; but the variables that define the cost relationships reported in Section 3 are quite general. Different sea-level rise distributions can be handled easily given the separable structure of Equations (3.5) and (3.6). Different protection cost assumptions can be considered (moving up to \$4000 per foot is ‘within sample’). Even property-value appreciation need not be driven by market forces to accommodate comparable analyses of the no-foresight case. Indeed, assumptions about a competitive market structure played a critical role only in factoring the effect of market-based adaptation with adequate foresight, coupled with a firm belief in both the sea-level forecasts and an announced policy of abandonment.



### Acknowledgement

This work was funded by the National Oceanic and Atmospheric Administration of the United States Department of Commerce through the Global Change Program, and the U.S. National Science Foundation and the Carbon Dioxide Research Program, Environmental Sciences Division of the U.S. Department of Energy under Grant ATM 95-22681. The authors also acknowledge the assistance offered in completing this work by James Neumann, Steven Swain and Ayman Ghanem.

### References

- Abraham, J. and Hendershott, P.: 1993, 'Patterns and Determinants of Metropolitan House Prices, 1977 to 1991', in Browne, L. E. and Rosengren, E. S. (eds.), *Real Estate and the Credit Crunch*, Proceedings of the Federal Reserve Bank of Boston, Boston, pp. 18–56.
- Bretherton, F. P., Bryan, K., and Woods, J. D.: 1990, 'Time-Dependent Greenhouse-Gas-Induced Climate Change', in Houghton, J. T., Jenkins, G. J., and Ephraums, J. J. (eds.), *Climatic Change: The IPCC Scientific Assessment*, Cambridge University Press, Cambridge, pp. 173–193.
- Brookshire, D., Thayer, M., Tschirhart, J., and Schulze, W.: 1985, 'A Test of the Expected Utility Model: Evidence from Earthquake Risk', *J. Pol. Econ.* **93**, 369–389.
- Charlson, R. J., Langner, J., Rodhe, H., Leovy, C. B., and Warren, S. G.: 1991, 'Perturbation of the Northern Hemisphere Radiative Balance by Backscattering from Anthropogenic Sulfate Aerosols', *Tellus* **43**, 152–163.
- Cline, W.: 1992, *The Economics of Global Warming*, Institute for International Economics, Washington, D.C., p. 399.
- Fankhauser, S.: 1994, 'Protection vs. Retreat: Estimating the Costs of Sea Level Rise', CSERGE, London.
- Hammitt, J. K., Lempert, R. J., and Schlesinger, M. E.: 1992, 'A Sequential-Decision Strategy for Abating Climate Change', *Nature* **357**, 315–318.
- Hoffert, M. I., Callegari, A. J., and Hsieh, C.-T.: 1980, 'The Role of Deep Sea Heat Storage in the Secular Response to Climatic Forcing', *J. Geophys. Res.* **85**, 6667–6679.
- Houghton, J. T., Callander, B. A., and Varney, S. K.: 1992, *Climate Change 1992, Supplementary Report to the IPCC Scientific Assessment*, Cambridge University Press, Cambridge, p. 200.
- Houghton, J. T., Meira Filho, L. G., Callander, B. A., Harris, N., Kattenberg, A., and Maskell, K. (eds.): 1996, *Climate Change 1995: The Science of Climate Change*, Cambridge University Press, Cambridge, p. 572.
- Lempert, R. J., Schlesinger, M. E., and Bankes, S. C.: 1996, 'When We Don't Know the Costs or the Benefits: Adaptive Strategies for Abating Climate Change', *Clim. Change* **33**, 235–274.
- Lempert, R. J., Schlesinger, M. E., and Hammitt, J. K.: 1994, 'The Impact of Potential Abrupt Climate Changes on Near-Term Policy Choices', *Clim. Change* **26**, 351–376.
- MacDonald, D., Murdoch, J., and White, H.: 1987, 'Uncertain Hazards, Insurance, and Consumer Choice: Evidence from Housing Markets', *Land Economics* **63**, 361–371.
- Nordhaus, W. D.: 1991, 'To Slow or Not to Slow', *Econ. J.* **5**, 920–937.
- Nordhaus, W. D.: 1994, *Managing the Global Commons: The Economics of Climate Change*, The MIT Press, Cambridge, p. 213.
- Nordhaus, W. D. and Yohe, G.: 1983, 'Future Paths of Energy and Carbon Dioxide Emissions', in *Changing Climate*, National Academy Press, Washington, D.C., pp. 87–152.
- Ramankutty, N.: 1994, *An Empirical Estimate of Climate Sensitivity*, M.S. Thesis, University of Illinois at Urbana-Champaign, p. 172.
- Schlesinger, M. E.: 1993, 'Greenhouse Policy', *Nat. Geogr. Res. Explor.* **9**, 159–172.
- Schlesinger, M. E. and Jiang, X.: 1991, 'Revised Projection of Future Greenhouse Warming', *Nature* **350**, 219–221.
- Schlesinger, M. E., Jiang, X., and Charlson, R. J.: 1992, 'Implication of Anthropogenic Atmospheric Sulphate for the Sensitivity of the Climate System', in Rosen, L. and Glasser, R. (eds.), *Climate*

- Change and Energy Policy: Proceedings of the International Conference on Global Climate Change: Its Mitigation through Improved Production and Use of Energy*, American Institute of Physics, New York, pp. 75–108.
- Schlesinger, M. E. and Ramankutty, N.: 1992, 'Implications for Global Warming of Intercycle Solar-Irradiance Variations', *Nature* **360**, 330–333.
- Schlesinger, M. E. and Ramankutty, N.: 1994a, 'An Oscillation in the Global Climate System of Period 65–70 Years', *Nature* **367**, 723–726.
- Schlesinger, M. E. and Ramankutty, N.: 1994b, 'Low-Frequency Oscillation. Reply', *Nature* **372**, 508–509.
- Schlesinger, M. E. and Ramankutty, N.: 1995, 'Is the Recently Reported 65–70 Year Surface-Temperature Oscillation the Result of Climatic Noise?', *J. Geophys. Res.* **100**, 13,767–13,774.
- Schneider, S. and Chen, R.: 1980, 'Carbon Dioxide Warming and Coastline Flooding: Physical Factors and Climatic Impact', *Ann. Rev. Energy* **5**, 107–140.
- Shine, K. P., Derwent, R. G., Wuebbles, D. J., and Morcrette, J.-J.: 1990, 'Radiative Forcing of Climate', in Houghton, J. T., Jenkins, G. J., and Ephraums, J. J. (eds.), *Climate Change: The IPCC Scientific Assessment*, Cambridge University Press, Cambridge, pp. 41–68.
- Smith, J. B.: 1996, 'Standardized Estimates of Climate Change Damages in the United States', *Clim. Change* **32**, 313–326.
- Smith, J. B. and Tirpak, D.: 1989, *The Potential Effects of Global Climate Change on the United States*, EPA-230-05-89-050, U.S. Environmental Protection Agency, Washington, D.C., p. 413.
- Titus, J. G. and Narayanan, V. K.: 1995, *The Probability of Sea Level Rise*, EPA 230-R-95-008, U.S. Environmental Protection Agency, Washington, D.C., p. 186.
- Warrick, R. A., Oerlemans, J., Woodworth, P. L., Meier, M. F., and le Provost, C.: 1996, 'Changes in Sea Level', in Houghton, J. T., Meira Filho, L. G., and Callander, B. A. (eds.), *Climatic Change 1995: The Science of Climate Change: Contribution of Working Group I to the Second Assessment Report of the IPCC*, Cambridge University Press, Cambridge, pp. 359–405.
- Weyant, J. P.: 1996, 'Second Round Results of the Energy Modeling Forum-14: Integrated Assessment of Climate Change', International Institute of Applied Systems Analysis, Stanford University mimeo, p. 48.
- Wigley, T. M. L. and Raper, S. C. B.: 1993, 'Future Changes in Global Mean Temperature and Sea Level', in Warrick, R. A., Barrow, E. M., and Wigley, T. M. L. (eds.), *Climate and Sea Level Change: Observations, Projections and Implications*, Cambridge University Press, Cambridge, pp. 111–133.
- Yohe, G.: 1989, 'The Cost of Not Holding Back the Sea – Economic Vulnerability', *Ocean Shoreline Manage.* **15**, 233–255.
- Yohe, G.: 1991, 'Selecting "Interesting" Scenarios with Which to Analyze Policy Response to Potential Climate Change', *Clim. Res.* **1**, 169–177.
- Yohe, G.: 1996, 'Exercises in Hedging against Extreme Consequences of Global Change and the Expected Value of Information', *Glob. Environ. Change* **6**, 87–101.
- Yohe, G., Neumann, J., Marshall, P., and Ameden, H.: 1996, 'The Economic Cost of Greenhouse-Induced Sea-Level Rise for Developed Property in the United States', *Clim. Change* **32**, 387–410.
- Yohe, G. and Wallace, R.: 1996, 'Near Term Mitigation Policy for Global Change under Uncertainty: Minimizing the Expected Cost of Meeting Unknown Concentration Thresholds', *Environ. Model. Assess.* **1**, 47–57.

(Received 13 January, 1997; in revised form 8 October, 1997)